



Protistan grazing impacts microbial communities and carbon cycling at deep-sea hydrothermal vents

Sarah K. Hu^{a,1} , Erica L. Herrera^a, Amy R. Smith^a , Maria G. Pachiadaki^b , Virginia P. Edgcomb^c , Sean P. Sylva^a , Eric W. Chan^d , Jeffrey S. Seewald^a , Christopher R. German^c , and Julie A. Huber^a

^aDepartment of Marine Chemistry and Geochemistry, Woods Hole Oceanographic Institution, Woods Hole, MA 02543; ^bDepartment of Biology, Woods Hole Oceanographic Institution, Woods Hole, MA 02543; ^cDepartment of Geology & Geophysics, Woods Hole Oceanographic Institution, Woods Hole, MA 02543; and ^dSchool of Earth, Environment, and Marine Sciences, The University of Texas Rio Grande Valley, Edinburg, TX 78539

Edited by David M. Karl, University of Hawaii at Mānoa, Honolulu, HI, and approved June 1, 2021 (received for review February 10, 2021)

Microbial eukaryotes (or protists) in marine ecosystems are a link between primary producers and all higher trophic levels, and the rate at which heterotrophic protistan grazers consume microbial prey is a key mechanism for carbon transport and recycling in microbial food webs. At deep-sea hydrothermal vents, chemosynthetic bacteria and archaea form the base of a food web that functions in the absence of sunlight, but the role of protistan grazers in these highly productive ecosystems is largely unexplored. Here, we pair grazing experiments with a molecular survey to quantify protistan grazing and to characterize the composition of vent-associated protists in low-temperature diffuse venting fluids from Gorda Ridge in the northeast Pacific Ocean. Results reveal protists exert higher predation pressure at vents compared to the surrounding deep seawater environment and may account for consuming 28 to 62% of the daily stock of prokaryotic biomass within discharging hydrothermal vent fluids. The vent-associated protistan community was more species rich relative to the background deep sea, and patterns in the distribution and co-occurrence of vent microbes provide additional insights into potential predator-prey interactions. Ciliates, followed by dinoflagellates, Syndiniales, rhizaria, and stramenopiles, dominated the vent protistan community and included bacterivorous species, species known to host symbionts, and parasites. Our findings provide an estimate of protistan grazing pressure within hydrothermal vent food webs, highlighting the important role that diverse protistan communities play in deep-sea carbon cycling.

deep-sea hydrothermal vents | microbial eukaryotes | predator-prey interactions | deep-sea food web ecology | protists

Mixing of hydrothermal vent fluids with surrounding seawater in the deep sea creates redox gradients that promote a hub of biological activity supported by chemosynthetic primary production in the absence of sunlight. These localized regions of elevated microbial biomass are important sources of carbon and energy to the surrounding deep-sea ecosystem (1–5). In particular, the consumption of hydrothermal vent microorganisms by single-celled microbial eukaryotes (or protists) is an important link in the food web in which carbon is transferred to higher trophic levels or remineralized to the microbial loop.

Protistan grazing is a significant source of mortality for bacterial and archaeal populations in aquatic ecosystems that also influences their composition and diversity (6). Assessments of grazing in the mesopelagic and dark ocean indicate that rates of consumption decrease with depth and correspond to bacterial abundance (7, 8). Therefore, at sites of increased biological activity and microbial biomass, such as areas of redox stratification, protistan grazing is higher relative to the rest of the water column (9, 10). Comparable data are lacking from deep-sea hydrothermal vents, in which the relatively high microbial biomass and rates of primary productivity suggest protistan grazing should be a significant source of microbial mortality and carbon transfer. Furthermore, single-celled microbial eukaryotes can serve as a nutritional resource for other larger protists and higher trophic levels (4, 11).

Early microscopic and culture-based experiments from several hydrothermal vents confirmed the presence of single-celled microbial eukaryotes, with observations and enrichment cultures revealing diverse assemblages of ciliates and flagellated protists (12, 13). The study of protistan taxonomy and distribution via genetic analyses at deep-sea vents has uncovered a community largely composed of alveolates, stramenopiles, and rhizaria (14–17). In addition to many of these sequence surveys identifying known bacterivorous species, ciliates isolated from Guaymas Basin were shown to consume an introduced prey analog (18). Collectively, these studies provide supporting evidence of a diverse community of active protistan grazers at deep-sea vents.

Here, we investigate protistan predation pressure upon microbial populations in venting fluids along the Gorda Ridge to test the hypothesis that protistan grazing and diversity is elevated within hydrothermal habitats compared to the surrounding deep sea due to increased prey availability. Estimates of mortality via protistan phagotrophy are calculated from grazing experiments conducted with low-temperature, diffusely venting fluid that mixes with seawater at and below the seafloor. Paired 18S ribosomal RNA (rRNA) gene amplicon sequencing from the same experimental sites and incubations reveals the *in situ* protistan diversity and distribution to evaluate potential preferences in prey, with a focus on the protistan grazer population and their relationship to bacteria and archaea. We present quantitative estimates of protistan grazing from a deep-sea hydrothermal vent ecosystem,

Significance

Heterotrophic protists are ubiquitous in all aquatic ecosystems and represent an important ecological link in food webs by transferring organic carbon from primary producers to higher trophic levels. Here, we quantify the predator-prey trophic interaction among protistan grazers and microbial prey within hydrothermal vent fluids from the Gorda Ridge spreading center in the northeast Pacific Ocean. Estimates of protistan grazing pressure were highest at sites of diffusely venting fluids, which are an oasis of biological activity in the deep sea. Our findings suggest that elevated grazing activity is attributed to a diverse assemblage of heterotrophic protistan species drawn to the hydrothermal vent habitat and demonstrates the important ecological roles that protists play in the deep-sea carbon cycle.

Author contributions: S.K.H., M.G.P., V.P.E., and J.A.H. designed research; S.K.H., E.L.H., A.R.S., S.P.S., E.W.C., J.S.S., C.R.G., and J.A.H. performed research and contributed to field operations; S.K.H., M.G.P., V.P.E., and E.W.C. contributed new reagents/analytic tools; S.K.H. analyzed data; and S.K.H. and J.A.H. wrote the paper.

The authors declare no competing interest.

This article is a PNAS Direct Submission.

Published under the PNAS license.

¹To whom correspondence may be addressed. Email: sarah.hu@whoi.edu.

This article contains supporting information online at <https://www.pnas.org/lookup/suppl/doi:10.1073/pnas.2102674118/-DCSupplemental>.

Published July 15, 2021.

thus providing details into the role protists play in food webs and carbon cycling in the deep sea.

Results and Discussion

Sea Cliff and Apollo Hydrothermal Vent Fields. Low-temperature (10 to 80 °C) diffusely venting fluids were collected at the Sea Cliff and Apollo hydrothermal vent fields along the Gorda Ridge (*SI Appendix, Fig. S1*) (19–21). Hydrothermal vent fluids collected for experiments and genetic analysis were geochemically distinct from plume (5 m above active venting), near-vent bottom water (lateral to venting fluid), and background seawater (outside the range of detectable hydrothermal influence; Table 1). The concentration of bacteria and archaea was 5 to 10×10^4 cells · mL⁻¹ in low-temperature vent fluids, which was higher than background seawater concentrations (3 to 5×10^4 cells · mL⁻¹; Table 1). Diffuse vents sampled in both fields represented a mixture of nearby high-temperature vent fluid (Candelabra, 298 °C and Sir Ventsalot, 292 °C) with seawater (22). During sample collection (30 to 40 min), the temperature of the fluid being sampled fluctuated between 3 to 72 °C, due to mixing (Table 1). The temperature maxima at Mt. Edwards and Venti Latte were lower compared to Candelabra and Sir Ventsalot and ranged from 11 to 40 °C; these sites also had visible tube worm clusters (*Ridgeia piscesae*; *SI Appendix, Fig. S1* and Table 1).

Protistan Grazers Exert Predation Pressure on Hydrothermal Vent Bacteria and Archaea. Grazing incubations conducted with fluids collected from five sites within the Sea Cliff and Apollo vent fields demonstrate that microbial eukaryotes actively graze microbial communities in hydrothermal vent fluids at an elevated rate relative to the surrounding deep-sea environment (Fig. 1). Protists consumed microbial prey at rates ranging between 700 to 1,828 cells · mL⁻¹ · hour⁻¹ in the diffuse venting fluids (Fig. 1B and *SI Appendix, Table S1*), whereas in near-vent bottom water away from active venting, the grazing rate was 255 cells · mL⁻¹ · hour⁻¹. The prokaryote turnover rate, expressed as the percentage of the daily consumed prokaryote biomass relative to the standing stock (average prokaryotic cell concentration), was 17.2% day⁻¹ in the bottom water near the hydrothermal vent sites. Protistan grazing at hydrothermal vents accounts for 28 to 62% of the daily prokaryote biomass turnover (Fig. 1C and *SI Appendix, Table S1*), demonstrating that the vent microbial community within discharging fluids is under more top-down pressure compared to communities in the background deep-sea environment.

Free-living heterotrophic protists may adapt to low prey encounter rates, due to decreased microbial biomass in the deep sea, by associating with sinking particles or localized habitats with more abundant prey (6, 23). Transition zones such as redoxclines often host a more abundant microbial population due to the presence of diverse sources of carbon and energy (9, 24); subsequently, these habitats are also sites of comparatively higher grazing pressure (grazing rate and prokaryote turnover) due to increased prey availability. In one of the only other studies to quantify deep-sea predation pressure, protistan grazing within a deep-sea halocline (3,500 m; above the hypersaline Urania Basin in the Eastern Mediterranean Sea) was calculated to be over 13,500 cells · mL⁻¹ · hour⁻¹, in contrast to 10 to 390 cells · mL⁻¹ · hour⁻¹ in the water column outside the influence of the halocline (100 to 3,000 m) (9). Near-vent bottom water grazing rates in our study (Fig. 1 and *SI Appendix, Table S1*) were comparable to rates previously obtained from mesopelagic and bathypelagic water column depths (200 to 2,500 m; ~10 to 400 cells · mL⁻¹ · hour⁻¹) (8, 10), while grazing rates and prokaryotic abundance were higher in vent fluids (Fig. 1 and *SI Appendix, Table S1*).

Commensurate with typical declining concentrations of prokaryotes with ocean depth, deep-sea grazing rates in this study were lower relative to those measured in seawater from euphotic regions (8, 9). However, when the microbial community abundance (cells · mL⁻¹) within diffuse flow fluids is taken into account, the impact of protistan grazing measured as a daily prokaryote turnover rate (28 to 62% · day⁻¹) at the hydrothermal vent sites are within the range of turnover rates reported from some euphotic zone studies (6). This observation is consistent with grazing rates reported from sub-euphotic depths, especially at environments with increased biological activity (reviewed in ref. 10).

Prokaryote turnover rates (percentage day⁻¹) were also found to be dependent on diffuse vent fluid temperature maxima ($r^2 = 0.87$; *SI Appendix, Fig. S4B*); otherwise, no other relationships between estimated grazing pressure and geochemistry were detected. While this trend is consistent with correlations between protistan grazing and temperature in previous euphotic zone studies (7, 25, 26), the lack of a relationship between temperature and grazing rate (both cells · mL⁻¹ · hour⁻¹ and µg of carbon · L⁻¹ · day⁻¹; *SI Appendix, Fig. S4B*) measurements, which are independent of estimated prokaryote cell abundances, suggests that there may be an indirect relationship between temperature and protist grazing activity involving the impact that temperature has on the growth and concentration of microbial prey populations.

Table 1. Chemical characteristics of the samples used in this study as well as nearby high-temperature end member fluid

Vent site	Depth (m)	Tmax (range) (°C)	pH	Mg (mM)	% Seawater (bag sample)	H ₂ S (mM)	H ₂ (µM)	CH ₄ (µM)	Microbial (cell · mL ⁻¹)
Sea cliff vent field									
Candelabra high-temperature vent	2,730	298	4.5	2.1	—	3	62.0	68.4	—
Candelabra diffuse vent	2,730	79 [9-68]	5.5 [5.8]	35.7 [45.8]	88.4%	n.d.	21.9	23.7	$5.51E \times 10^4$
Candelabra plume	2,725	1.7	—	—	—	—	—	—	$7.69E \times 10^4$
Venti Latte vent	2,708	11 [10-23]	6.4 [5.5]	50.9 [50.4]	97.3%	n.d.	b.d.	0.9	$1.11E \times 10^4$
Mt Edwards vent	2,707	40 [15-30]	6.0 [5.8]	42.6 [42.8]	82.5%	1.01	127.0	10.1	$5.14E \times 10^4$
Mt Edwards plume	2,702	1.8	—	—	—	—	—	—	—
Apollo vent field									
Sir Ventsalot high-temperature vent	2,732	292	2.8	2.5	—	2.53	71.4	66.7	—
Sir Ventsalot diffuse vent	2,732	[3-72]	n.d.	50.8	98.0%	—	—	—	$5.30E \times 10^4$
Background									
Near-vent bottom water	2,745	1.7	7.8	51.8	100%	—	—	—	$5.20E \times 10^4$
Seawater: shallow	150	8.6	n.d.	51.8	100%	—	—	—	—
Seawater: deep	2,010 to 2,090	1.8	7.8	51.8	100%	—	—	—	$3.91E \times 10^4$

n.d., no data; b.d., below detection. For vents sampled with both the SUPR and IGT, data in brackets are from SUPR bag samples used in grazing experiments, whereas all other data are from paired IGT samples at the same site. Sir Ventsalot was only sampled via SUPR. For plume and seawater samples, data are from Niskin bottles.

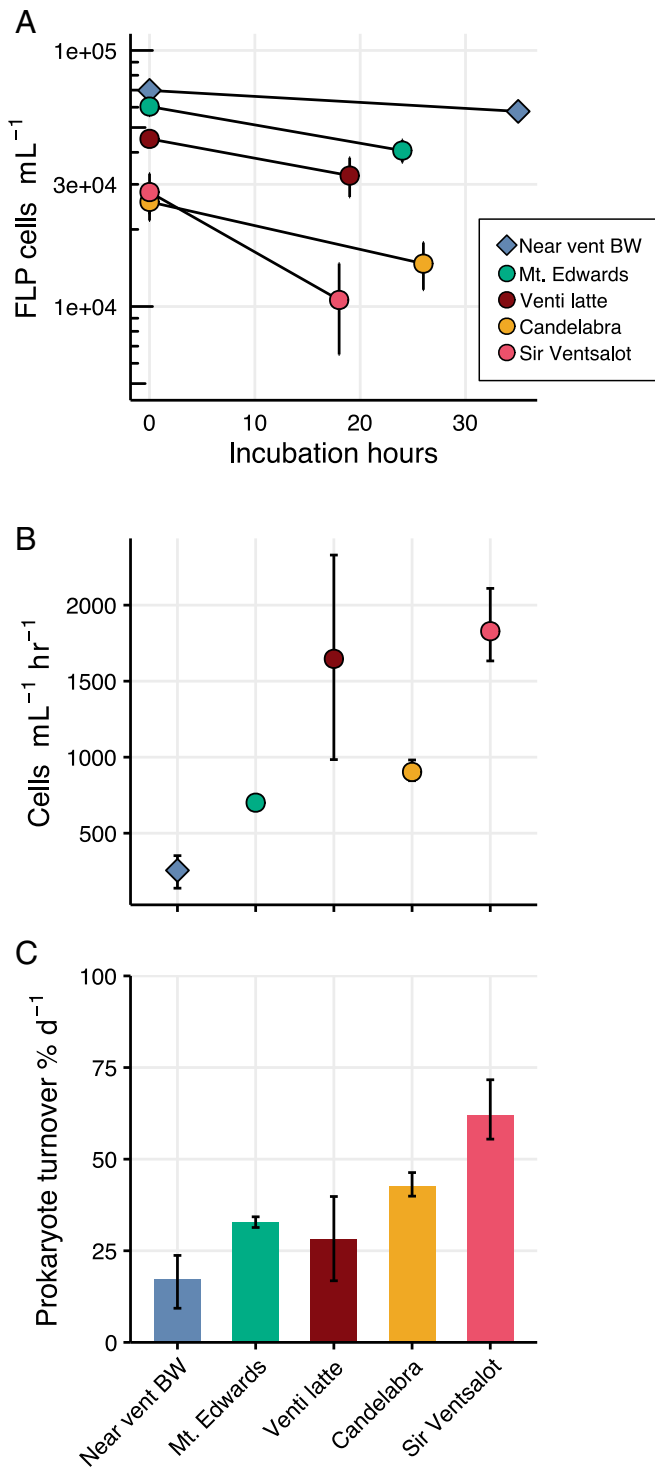


Fig. 1. Results from grazing experiments conducted at Sea Cliff and Apollo hydrothermal vent fields. (A) Loss of FLP (log $\text{FLP cells} \cdot \text{mL}^{-1}$; y-axis) during each incubation (hours; x-axis). Error bars represent the standard mean error from the average across replicates. (B) Grazing rate for each site expressed as the consumption of $\text{cells} \cdot \text{mL}^{-1} \cdot \text{hour}^{-1}$, derived from Eq. 1. Error bars report the minimum and maximum grazing rate derived from the standard mean error. (C) Estimated daily prokaryote turnover percentage ($\% \text{ d}^{-1}$), in which the grazing rate for each site was multiplied by the in situ prokaryote cell concentration (Table 1). Error bars represent the minimum and maximum derived from the range of grazing rate for each incubation. Complete experiment details are reported in *SI Appendix, Table S1*.

Grazing rates from Sea Cliff and Apollo vent fields indicate that protists may be consuming or remineralizing 1.45 to 3.77 μg of carbon $\cdot \text{L}^{-1} \cdot \text{day}^{-1}$ [*SI Appendix, Table S1*; using a carbon conversion factor of 86 fg carbon $\cdot \text{cell}^{-1}$ (27)]. While few measurements of absolute fixed carbon exist from hydrothermal vents, McNichol et al. estimate primary production of the microbial community associated with low-temperature diffuse fluids at the East Pacific Rise to range between 17.3 to 321.4 $\mu\text{g C} \cdot \text{L}^{-1} \cdot \text{day}^{-1}$, at 24 °C and 50 °C under in situ pressure, representing an important source of new labile carbon in the deep sea (2, 3). Considering these estimates, protistan grazing may account for the consumption or transformation of up to 22% of carbon fixed by the chemosynthetic population in discharging vent fluids. While the eventual fate of this carbon remains unconstrained, protistan grazing will release a portion of the organic carbon into the microbial loop as a result of excretion, egestion, and sloppy feeding, while another proportion will be taken up by larger organisms that consume protistan cells. In prior work, it has been shown that carbon fixed within hydrothermal vent plumes and exported to the underlying seafloor has the potential to outweigh the flux of sinking organic carbon that persists to depth from the overlying surface ocean (1); our work illustrates previously unquantified pathways by which protistan grazing activity may also contribute to carbon cycling in hydrothermal ecosystems. Our findings show that the trophic exchange between microbial prey and activities of protistan grazers at hydrothermal vents is significant and may account for a substantial amount of organic carbon transfer at the base of deep-sea food webs.

Distinct Microbial Populations at Hydrothermal Vents. The Sea Cliff and Apollo hydrothermal vent sites were found to host a diverse assemblage of protists (Figs. 2A and 3). Amplicon sequencing of the protistan (18S rRNA gene) and prokaryotic (16S rRNA gene) communities resulted in 9,027 and 6,497 amplicon sequence variants (ASVs), respectively. ASVs represent approximately species- or strain-level designations based on recovered sequences (*SI Appendix*). The taxonomic composition of 18S rRNA gene-derived ASVs reveal dominant members of the vent ecosystem to include ciliates, dinoflagellates, Syndiniales, rhizaria, and stramenopiles (Fig. 2A); these same protistan groups are enriched in other deep-sea niche habitats, such as methane seeps and other hydrothermal vent systems or vent fluid-influenced environments (14, 15, 17, 18, 28). Community-wide analyses of both protists (18S rRNA gene amplicons) and bacteria and archaea (16S rRNA gene amplicons) showed that replicate samples cluster together (Fig. 2B and *SI Appendix, Figs. S5 and S6 and SI Appendix*). Background, plume, and near-vent bottom water bacteria and archaea community compositions were distinct from the vent-associated community (*SI Appendix, Fig. S6*). Sites of actively venting fluid hosted higher relative sequence abundances assigned to the *Epsilonbacteraeota* class, including *Sulfurimonas* and *Sulfurovum* (*SI Appendix, Fig. S6A*), which are commonly dominant within vent microbial communities (29). The expected impact of vent fluid collection and depressurization was evidenced by differences in the protistan community composition in samples from in situ (Suspended Particle Rosette Sampler [SUPR] or sterivex filters) and the start of each grazing experiment (T_0 ; Fig. 2A) (30). However, consistency among grazing experiment sample community composition and ordination analysis demonstrated that the collected vent fluid used for grazing incubations was representative of the hydrothermally-influenced community (Fig. 2A and B).

To test the hypothesis that microbial eukaryotes from the surrounding deep-sea environment have greater species richness at sites of low-temperature diffuse venting, ASVs were classified based on their distribution within and across vent fluid and non-hydrothermally influenced environments (background). “Resident” ASVs were found only within hydrothermally influenced samples and considered to be potentially vent endemic, and “cosmopolitan”

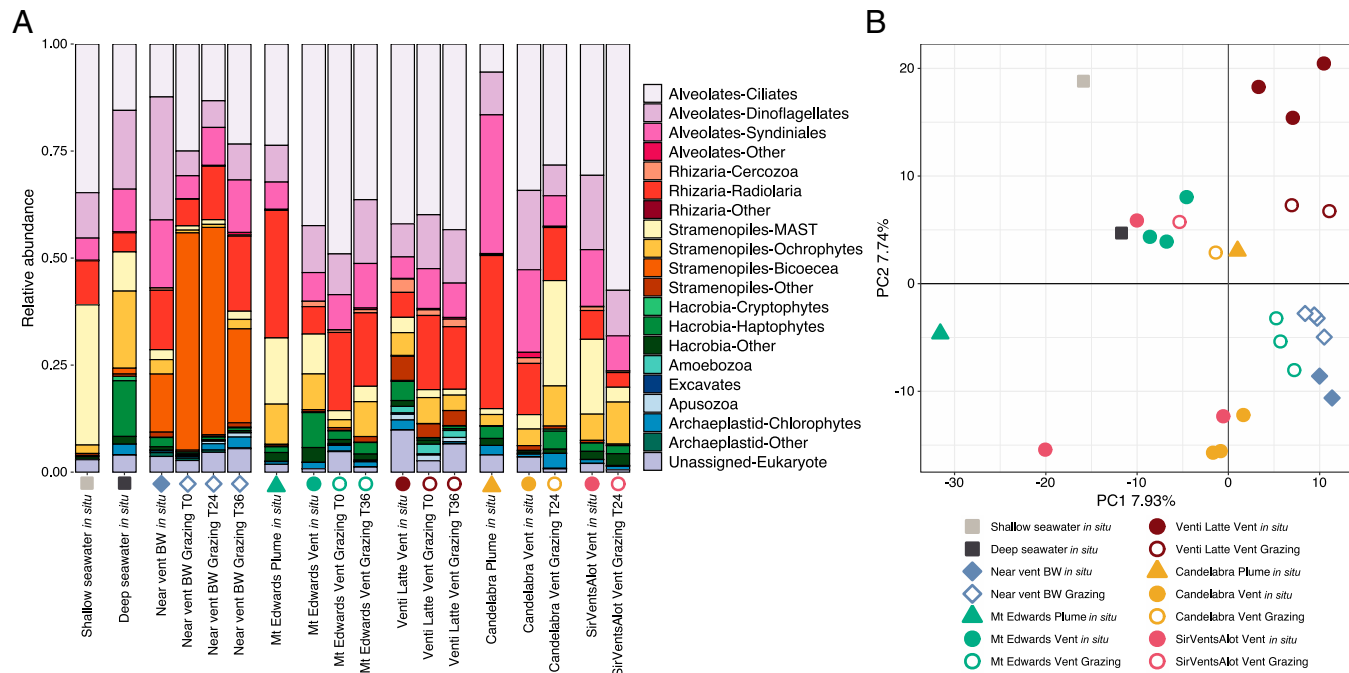


Fig. 2. Summary of protistan diversity for in situ and grazing experiment samples. (A) Taxonomic breakdown of samples, including background, plume (5 m above active flow), near-vent bottom water (BW), in situ vent sites, and associated grazing incubation bottles (T_x). Bar plot reports the relative sequence abundances, in which colors designate major protistan taxonomic groups (based on manual curation; Materials and Methods). (B) Ordination analysis of all samples, including replicates, from the 18S rRNA gene-derived sequence data. Data were center log-ratio transformed ahead of principle components analysis. For both A and B, symbols indicate origin of sample, and color denotes vent site. Solid symbols represent in situ samples, and open symbols designate samples from grazing experiments. Samples from grazing experiments include different time points (SI Appendix, Table S1).

ASVs included those detected throughout the background and hydrothermally influenced samples (SI Appendix and SI Appendix, Fig. S7). The total number of ASVs within the resident population was several-fold higher than in the cosmopolitan population (4,236 resident versus 535 cosmopolitan ASVs), yet the number of sequences assigned to each population was similar (48% cosmopolitan and 46% resident). An 18S rRNA gene survey comparing Mariana Arc vent fluids with the background environment similarly found species richness to be higher within the vent-only protistan population (17). While biases with sequence-based analyses inhibit our ability to infer absolute abundances and do not necessarily provide full coverage of the entire microbial community, results from these molecular surveys support the hypothesis that protistan diversity is enriched (higher species richness) within hydrothermal vent mixing zones relative to the surrounding deep-sea environment. The niche habitat created by the discharging fluids mixing with the surrounding seawater likely contributes to supporting an increased abundance of bacteria and archaea (Table 1) and, consequently, attracts a diverse community of protistan heterotrophs that ultimately places top-down pressure on the microbial population (Figs. 1 and 2 and SI Appendix, Table S1).

To assess the composition of the putative grazer population, we closely examined the diversity and distribution of key protistan lineages known to exhibit heterotrophy in other environments (SI Appendix and Datasets S2–S4). Ciliates were identified as important grazers in the hydrothermal vent fluids from these sites, as many groups detected include well-known bacterivorous species (31). The Oligohymenophorea and Spirotrichea classes had particularly higher species richness within the Gorda Ridge vent fluids (Fig. 3), and species within these groups may be specially suited to thrive within the vent environment. For example, scuticociliates (a subclass within Oligohymenophorea; Dataset S4) have previously been found near hydrothermal vent sites (28, 32) and, in addition to their heterotrophic capabilities, are known to be

parasitic or to host endosymbionts (31). Ciliates found only within the vent fluid samples, such as Karyorelictea, Plagiopylea, and *Euplotia*, include species capable of thriving in low oxygen to suboxic environments with modified mitochondria (hydrogenosomes) and form symbiotic relationships with methanogens or bacteria (33, 34). Taxonomic groups within ciliates and other alveolates, rhizaria (radiolaria and cercozoa), amoebozoa, apusozoa, and excavates that were detected primarily in the resident population (Fig. 3) include species that are candidates in future efforts to understand the functional traits among hydrothermal vent endemic protists; many of these same groups were previously identified as vent endemic species along the Mariana Arc (17). Heterotrophic nanoflagellate members of the stramenopile supergroup were overwhelmingly MArine STramenopiles (MAST, in cosmopolitan and resident populations) or *Cafeteriaeae* (primarily in the near vent bottom water samples) (Fig. 3); both are recognized as important bacterivores with a global distribution and often found in mesopelagic and deep-sea surveys (35–37). MAST have also been found at higher relative sequence abundances within the Mariana Arc vent ecosystem and hydrothermally influenced water masses within Okinawa Trough (17, 28).

We also found evidence for parasitic populations of protists that may represent a source of mortality to the protists themselves and other small eukaryotes (e.g., metazoa) in venting fluids from the Gorda Ridge. Parasitic protists have been found to account for a significant portion of the globally distributed heterotrophic protistan community (38), in which the most abundant genetic signatures were affiliated with Syndiniales (also marine alveolate). Syndiniales are also recognized as a major source of mortality for many microbial eukaryotes as well as metazoa and are typically found in association with ciliates, dinoflagellates, and rhizaria (39); our data suggest they may also represent a source of mortality among the vent protistan population (Dino Groups I to V; Fig. 3). The prevalence of Syndiniales, along with other protistan lineages

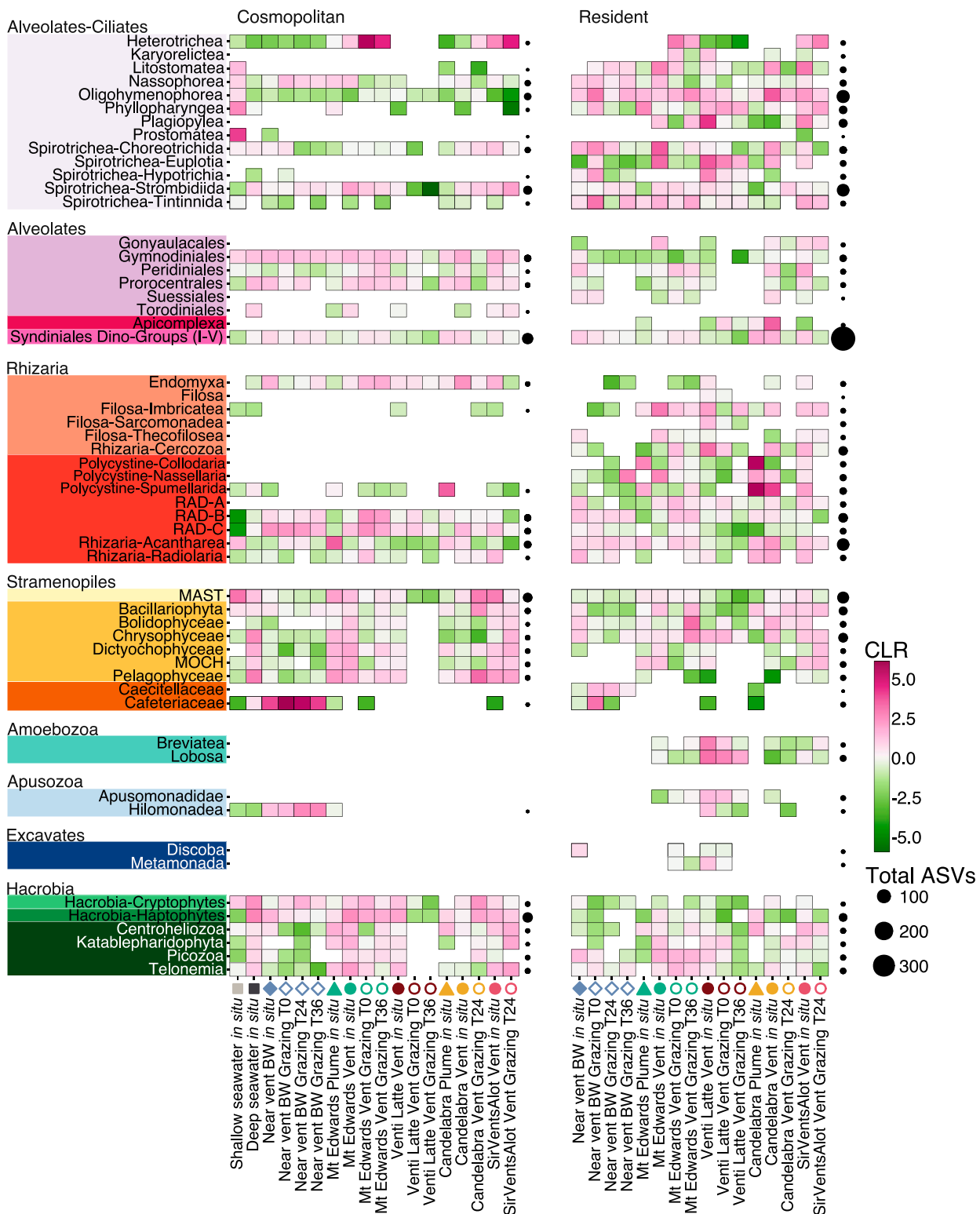


Fig. 3. Prevalence, distribution, and richness of protists at the class or order level across all samples. Centered log-ratio (CLR) transformed sequence abundances (green to pink heat map) for all samples, including background, in situ, plume, and grazing incubations (columns; x-axis) are shown by taxonomic group (color schema by row; y-axis), and classification as either cosmopolitan (Left) or resident (Right). CLR value is a result of transforming the sequence counts, so the geometric mean equates to 0. Ahead of sequence transformation, sequences within an ASV were averaged across replicates, then sequences were summed at approximately the class or order level (y-axis). Blank spaces indicate that no sequences were detected. Bubble plots to the right of each panel represent the total number of ASVs (by size) for the distribution (cosmopolitan versus resident) for each row.

known to include parasitic species (e.g., ciliates, amoebae, or cercozoa), supports previous observations that parasitism is widespread and likely contributes to carbon turnover in deep-sea food webs (40). Parasitism and grazing by microbial eukaryotes, along with other modes of microbial mortality such as viral lysis, should be included in future studies of deep-sea food web ecology.

Network analysis (41) based on a subset of the 18S and 16S rRNA gene-derived ASVs was used to query putative predator-prey interactions in this study. While results do not confirm the exact preferred prey preferences among hydrothermal vent protistan consumers, results identify significantly co-occurring instances of protists and bacteria or archaea (Fig. 4; compare links between inner and outer circles). Within the Gorda Ridge protistan assemblage, a higher proportion of the interactions associated with the resident protistan population was among ciliates (Fig. 4B). The most common interactions with the putative ciliate grazer population were with the most abundant prokaryotic groups (Fig. 4), including *Alphaproteobacteria*, *Gammaproteobacteria*, *Nitrososphaeria*, and *Sulfurimonas*. Inferred predator-prey relationships from this study represent hypotheses for future efforts to characterize protistan grazing preferences within the hydrothermal vent food web. Identifying these interactions is of ecological importance, because protistan grazers can place selective pressures on the prey species community composition; protists may preferentially consume cells based on their morphology or nutritional value (reviewed in refs. 42 and 43). For instance, if protist grazers favored small cell sizes, grazing activity may shift the microbial community suspended within the diffuse fluid toward larger cell types or cells that form aggregates or filaments (44, 45). In order to accurately capture predator-prey interactions *in situ* and understand the selective pressures grazing may place on the microbial prey community structure, future studies need to consider the diverse modes of protistan feeding and suitability of preferred prey types.

Reported grazing rates in this study quantify the impact of protistan grazing on microbial prey within low-temperature diffuse hydrothermal vent fluids. Findings from our paired quantitative and qualitative approach provide insight into the ecological roles of protists at deep-sea vents and their subsequent impact on the deep-sea carbon budget through carbon trophic transfer and release of dissolved organic matter. Phagotrophic grazing on smaller microorganisms accounts for a considerable amount of mortality in many aquatic environments and undoubtedly influences the diversity and composition of the hydrothermal vent diffuse flow microbial community; thus, efforts to fully characterize the microbial loop in the deep sea should include the roles of microbial eukaryotes. Protistan grazing is a key route of carbon transformation and exchange in the hydrothermal vent food web, and these findings contribute to our growing understanding of carbon cycling in the deep ocean.

Materials and Methods

Sample Collection and Processing. The Gorda Ridge spreading center, located ~200 km off the coast of southern Oregon, was visited in May through June 2019 with the E/V Nautilus (cruise NA108) (20). Low-temperature diffuse hydrothermal vent fluid samples <100 °C were collected using the remotely operated vehicle (ROV) *Hercules* and a SUPR (46). This involved measuring the fluid temperature with the Hercules temperature probe in regions of hydrothermal fluid flow then positioning the sampler intake into the vent for collection of discharging fluid. The SUPR sampler pumped fluid to either fill gas-tight bags (PET/METPET/LLDPE; ProAmpac, Rochester, NY) with 2 to 6 L of vent fluid for processing shipboard or to filter between 4.1 and 6.6 L of fluid through a 142-mm, 0.2-μm polyethersulfone (PES) filter (MilliporeSigma) for *in situ* samples. Filling and filtering rates ranged between 0.3 to 1.3 L · min⁻¹. Fluid was also collected by Niskin bottles mounted on the port forward side of the ROV within the vicinity of the hydrothermal vent but outside of the range of venting fluid (near vent bottom water) at 2,745 m and within the plume by situating the ROV ~5 m above an active venting site. Background seawater from the water column at ~2,100 m was

also obtained by a Niskin bottle. Upon retrieval, filters from the SUPR sampler were stored in RNAlater (Ambion) for 18 h at 4 °C then moved to -80 °C. Niskin samples from the plume and background were emptied into acid-washed cubitainers. Fluids from bags and cubitainers were sampled for prokaryote cell counts by preserving fluid with formaldehyde (1% final concentration). Excess fluid from each bag was also filtered onto sterivex filters (0.2 μm; MilliporeSigma) and stored with RNAlater identically to the *in situ* filters.

Whenever possible, the same vent fluids and high-temperature end-members were also sampled with Isobaric Gas Tight samplers (IGTs) (47) for geochemical analyses, which were processed immediately after recovery of the ROV. Shipboard analyses included pH measured at room temperature (25 °C) using a Ag/AgCl combination reference electrode, dissolved H₂ and CH₄ by gas chromatography with thermal conductivity detection following headspace extraction, and total aqueous sulfide ($\Sigma\text{H}_2\text{S} = \text{H}_2\text{S} + \text{HS}^- + \text{S}^{2-}$) following aqueous precipitation as Ag₂S for subsequent gravimetric determination in a shore-based laboratory. Aliquots of fluid were stored in 30 mL serum vials and acid-cleaned Nalgene bottles for shore-based measurement of total dissolved carbonate ($\Sigma\text{CO}_2 = \text{H}_2\text{CO}_3^* + \text{HCO}_3^- + \text{CO}_3^{2-}$) by gas chromatography and Mg by ion chromatography, respectively.

Grazing Experimental Procedure. Stocks of Fluorescently Labeled Prey (FLP) were prepared using a modified protocol from (48) with monocultures of *Hydrogenovibrio* (Strain MBA27) (49); preparation of FLP prey analog is described in the *SI Appendix*. The prey type was specifically chosen as a hydrothermal vent representative isolate and was found to have a similar size and morphology to resident bacteria (*SI Appendix*, Fig. S1). FLP stained with 5-(4,6-dichlorotriazinyl) aminofluorescein (DTAF) are nontoxic to consumers, and upon digestion, the DTAF label disappears (48).

Grazing experimental setup and execution followed the guidelines in Caron (50) with modifications described below (*SI Appendix*, Fig. S2). A summary of grazing experiments including site, vent name, depth, incubation temperatures, start times, and sampling time points can be found in *SI Appendix*, Table S1. Vent fluid collected from gas-tight bags was first filtered through 300 μm mesh to remove large multicellular metazoa and transferred into acid-washed and clean 500-mL plastic bottles using a peristaltic pump. Controls were prepared by filtering the fluid through a 0.2-μm filter to ensure that the FLP tracer did not disappear over the course of the experiment in the absence of grazers. Experiments were conducted in duplicate or triplicate, and controls were conducted in duplicate (*SI Appendix*, Fig. S2). FLP were added at concentrations 50% greater than the *in situ* microbial population, as there were no prior estimates of microbial concentrations or the ability to count cells onboard before the initiation of the experiments (*SI Appendix*, Table S1). The suggested amount of labeled prey to be added is between 1 and 10% of *in situ* microbial concentration (50); thus, the higher amount given during these incubations has probably led to overestimation of the estimated rates. Samples at T₀ were collected for cell counts following addition of FLP and gently mixing by fixing 10 mL of fluid in cold formaldehyde at a final concentration of 1%. Collected fluid in bags (vents) or Niskin bottles (background) remained on the ROV for several hours before the start of each shipboard incubation; thus, to minimize additional temperature changes and keep incubation conditions consistent between all experiments, bottles were placed in a dark cooler for incubation, in which temperatures ranged between 12 and 17 °C (*SI Appendix*, Table S1). In addition to other potential artifacts of bottle-based grazing experiments (i.e., pressure differences, sample handling, and bottle effect), we acknowledge that incubation temperatures for the grazing experiments were lower than the *in situ* discharging hydrothermal vent fluid and higher than the measured background seawater environment, which may have contributed to an underestimate or overestimate of grazing rates, respectively.

Grazing incubations were run for a total of 24 to 48 h, during which sample fluid for FLP counts was preserved with formaldehyde at two time points (T₁ and T₂, *SI Appendix*, Table S1). To assess the composition of protistan grazers in grazing incubations via molecular analysis, samples at each time point were vacuum filtered onto 0.2-μm PES filters (Millipore Express), stored with RNAlater at 4 °C overnight, and frozen at -80 °C. These were collected in duplicate when possible, and the volume filtered ranged from 0.9 to 2.7 L (*SI Appendix*, Table S1 and Fig. S2). In some cases, a T₀ sample was taken after addition of FLP and before incubation started, providing an assessment of the degree to which the community composition in the initial water samples was altered by sample handling between collection *in situ* and initiation of the experiments shipboard. A molecular sample at T₀ was not always collected (e.g., Candelabra and Sir Ventsalot), and a subset of grazing

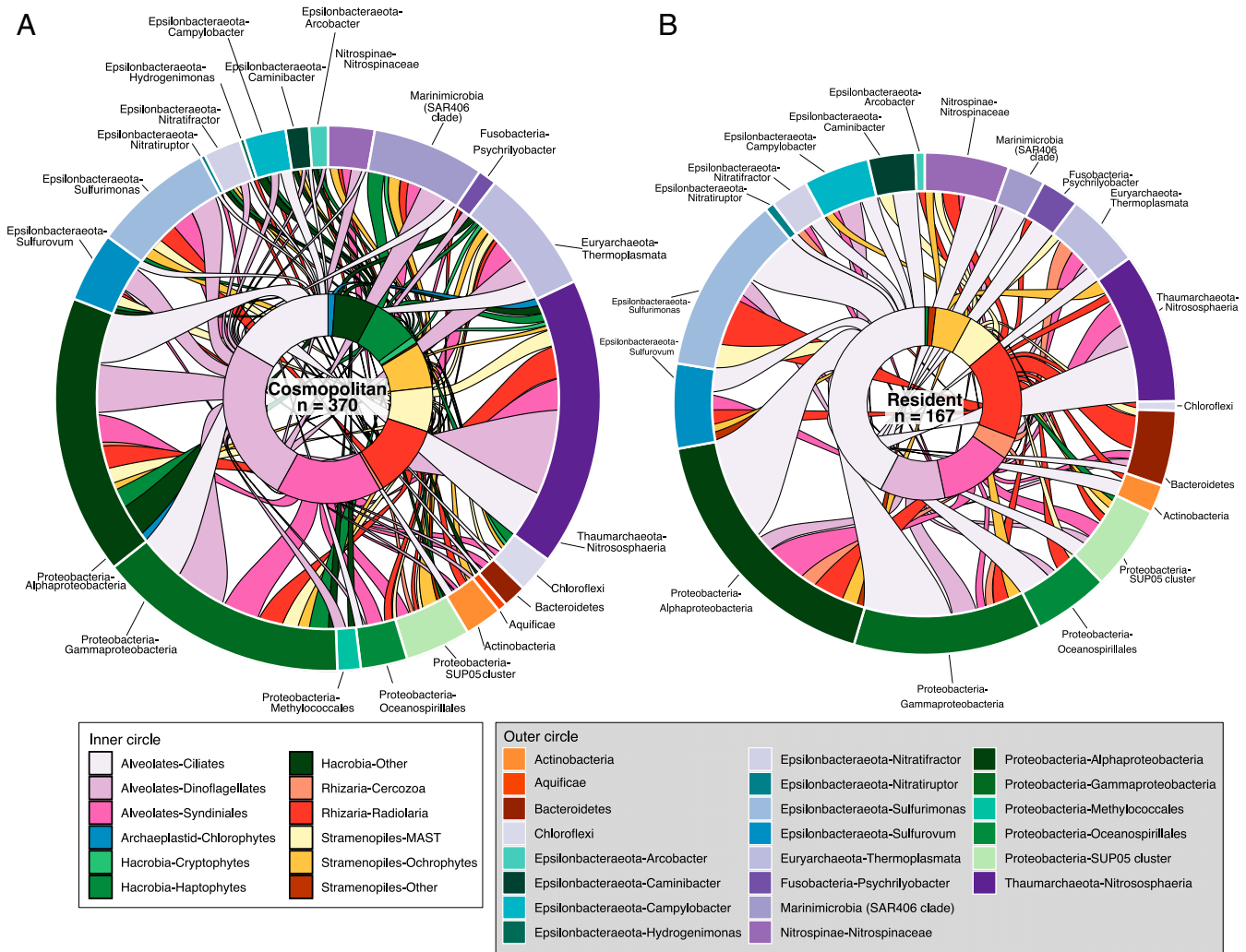


Fig. 4. Alluvial representation of the interaction between protists (inner circle) and bacteria or archaea (outer circle) derived from the SPIEC-EASI network analysis (Materials and Methods). The total number of interactions for the (A) cosmopolitan protist population ($n = 370$) was greater than the number of interactions involving the (B) resident protist population ($n = 167$). The color of the inner circle and alluvials that connect the inner to outer circle designate the protist taxonomic group (derived from 18S rRNA ASVs), and the color of the outer circle represents the bacteria or archaea group (derived from the 16S rRNA ASVs). Significant 18S–16S ASV pairs are listed in [Dataset S5](#); here, those ASV pairs were summed together based on membership to the protist or prokaryotic taxonomic groups.

experiments was conducted at different time points ranging from 18 to 36 h ([SI Appendix, Table S1](#)).

To track the disappearance of FLP over time, triplicate slides were prepared from each time point in a shore-based laboratory by filtering 2 to 4 mL of preserved fluid from each time onto 0.2- μ m black polycarbonate filters. Following filtration, 10 to 15 μ L of a stain solution made with 4',6-diamidino-2-phenylindole (DAPI; ~ 10 μ g/mL; [SI Appendix](#)) was gently piped onto the filter and covered with a coverslip. Experimental and control slides were counted using epifluorescence microscopy within 1 to 2 d and stored at 4 °C. FLPs were counted under the fluorescein isothiocyanate filter at 100 \times or 63 \times ; 16 fields of view were counted, and the cell mL^{-1} concentration was determined from this value for each slide. The technical error rate was calculated by taking the percentage of the SD over the mean for replicate counts. This technical error rate percentage was used to set the threshold at which a change in FLP abundance over time was considered true (i.e., if the percent change in FLP from T_0 to T_1 did not exceed the technical error rate, the loss of FLP by T_1 was not considered significantly different from T_0).

The concentration of FLPs at each time point was averaged across replicates. The difference in FLP concentration ($\text{cells} \cdot \text{mL}^{-1}$) from T_0 and T_F was used to estimate the number of cells grazed (G). For each experiment, T_1 or T_2 was chosen as T_F , when the loss in FLP exceeded the technical error rate. In the case in which both T_1 and T_2 exceeded the range of error, T_1 was chosen

as T_F ([SI Appendix, Fig. S3](#)). Using a model described in Salat and Marrasé (51) the number of cells grazed by protists (G) was estimated using the equation:

$$G = (T_0 - T_F) \left(\frac{N_0}{T_0} \right), \quad [1]$$

where T_0 and T_F equal the average FLP concentrations at the beginning and end of the experiment and N_0 equals the concentration of in situ prokaryote cell concentration (51). This model assumes that the ratio of FLP to in situ microbial prey remains consistent. The grazing rate was calculated by normalizing G to time at T_F ($\text{cells} \cdot \text{mL}^{-1} \cdot \text{hour}^{-1}$). The daily prokaryote turnover percentage was calculated by multiplying the in situ prokaryote cell concentration (taken at T_0) by the estimated grazing rate per day (9, 51). Grazing rates were converted to measures of carbon biomass using the assumption that the amount of carbon per prey cell is 86 fg C [Morono et al. (27); [SI Appendix, Table S1](#)].

Eukaryotic Molecular Sample Processing. Samples collected for molecular analyses included in situ filters from the SUPR sampler, shipboard sterilized filters, or time points from grazing experiments (all collected into 0.2- μ m pore size filters; MilliporeSigma). RNA was extracted and the 18S rRNA gene was reverse-transcribed to make complementary DNA; the V4 hypervariable region (52) was amplified according to Hu et al. (53) ([protocols.io](#); <http://dx.doi.org/10.17504/protocols.io.hk3b4yn>) and as described in [SI Appendix](#). Samples were

multiplexed, pooled at equimolar concentrations, and sequenced with the MiSeq 300 × 300 bp paired end kit at the Marine Biological Laboratory Bay Paul Center sequencing facility.

Prokaryotic Sample Processing. Prokaryotic cells were enumerated in formaldehyde-fixed fluids using DAPI (*SI Appendix*). DNA was extracted from PES filters or sterivex filters (0.2 µm) as described in ref. 54 and *SI Appendix*. 16S rRNA gene amplicon libraries were prepared and sequenced by the University of Connecticut Microbial Analysis, Resources, and Services using modified Earth Microbiome Project 16S rRNA gene V4 primers 515F and 806R (55–58).

Sequence Analysis. All sequences were quality controlled and processed in QIIME2 (version 2019.4) (59). Chimeric sequences were removed (pooled) and ASVs were determined with DADA2 (60). ASVs from 18S rRNA amplicons were assigned taxonomy using the Protist Ribosomal 2 Database (version 4.12; <https://github.com/pr2database/pr2database>) (61). Taxonomy assignment was performed with the naive Bayesian classifier method in the DADA2 R package with a minimum bootstrap of 70 (60, 62). Removal of contaminant 18S rRNA sequences is described in *SI Appendix*. For 16S rRNA gene-derived ASVs, the SILVA database (version 132) (63) was used for taxonomy assignment.

Molecular samples from *in situ* filters and shipboard sterivex filters were treated as replicates, in which sequence counts were averaged across replicates at the ASV level. ASV taxonomy assignment for both the 18S rRNA and 16S rRNA gene was manually curated and visualized to highlight the main taxonomic groups (*SI Appendix*). Due to the compositional nature of tag-sequence datasets, data were transformed by center log-ratio ahead of principle component analysis (PCA) and to visualize ASV-level changes across samples (64, 65).

To detect possible microbial interactions, Sparse InversE Covariance estimation for Ecological Association and Statistical Inference (SPIEC-EASI) analysis was performed using the cross-domain approach with ASVs from 18S rRNA and 16S rRNA gene results (66). SPIEC-EASI is designed to minimize spurious ASV-ASV interactions that result from the influence of compositional nature of tag-sequencing results (41). Only *in situ* samples that were found in both the 18S rRNA and 16S rRNA gene amplicon results were considered for the network analysis. Both datasets were subsampled to

include ASVs that appeared in at least three samples, had at least 50 sequences each, and made up at least 0.001% of the sequenced reads. 18S rRNA and 16S rRNA gene datasets were each center log-ratio transformed, then SPIEC-EASI was run using the Meinshausen–Buhmann's neighborhood selection estimation method. Significant interactions to infer putative predator–prey relationships were determined by subsetting only interactions between 18S rRNA– and 16S rRNA–derived ASVs.

Data Availability. A complete compilation of code to reproduce all analyses is available at GitHub, <https://shu251.github.io/protist-gordaridge-2021/> (67). A GitHub repository also includes raw microscopy count results, raw sequence count information, and ASV tables (<https://github.com/shu251/protist-gordaridge-2021>) (68). Both 18S rRNA and 16S rRNA amplicon sequences have been deposited in the Sequence Read Archive under BioProject **PRJNA637089** (**Dataset S1**). All other study data are included in the article and/or supporting information.

ACKNOWLEDGMENTS. We would like to thank Chip Breier, Darlene Lim, and Nicole Raineault for their contributions to the field operations. We would also like to extend gratitude to David Caron, Paige (Connell) Hu, Susanne Menden-Deuer, Roxanne Beinart, and Alexis Pasulka for helpful conversation and discussion regarding grazing experiments and deep-sea protistan diversity and to Jesse McNichol for discussion of carbon fixation rates. Margrethe Serres and Patrick Carter provided laboratory support for preparation of FLP. This research was supported by the NASA Planetary Science and Technology Through Analog Research (PSTAR) Program (NNH16ZDA001N-PSTAR) grant (16-PSTAR16_2-0011), National Oceanic and Atmospheric Administration (NOAA) Office of Ocean Exploration and Research, Ocean Exploration Trust, and NOAA-OER Grant NA17OAR0110336, and the Charles E. Hollister Endowed Fund for Support of Innovative Research at Woods Hole Oceanographic Institution (WHOI). This research used samples and data provided by the Ocean Exploration Trust's Nautilus Exploration Program, Cruise NA108. E.L.H. was supported by the WHOI Summer Student Fellowship and NSF Research Experiences for Undergraduates (REU) (OCE-1852460). The NSF Center for Dark Energy Biosphere Investigations (C-DEBI) supported J.A.H. as well as S.K.H. through a C-DEBI Postdoctoral Fellowship (OCE-0939564). Research and analysis were also supported through an NSF grant (OCE-1947776) awarded to J.A.H. and M.G.P. This is SUBSEA Publication Number SUBSEA-2021-001 and C-DEBI contribution number 568.

1. C. R. German *et al.*, Hydrothermal Fe cycling and deep ocean organic carbon scavenging: Model-based evidence for significant POC supply to seafloor sediments. *Earth Planet. Sci. Lett.* **419**, 143–153 (2015).
2. N. Le Bris *et al.*, Hydrothermal energy transfer and organic carbon production at the deep seafloor. *Front. Mar. Sci.* **5**, 531 (2019).
3. J. McNichol *et al.*, Primary productivity below the seafloor at deep-sea hot springs. *Proc. Natl. Acad. Sci. U.S.A.* **115**, 6756–6761 (2018).
4. S. A. Bennett *et al.*, Trophic regions of a hydrothermal plume dispersing away from an ultramafic-hosted vent-system: Von Damm vent-site, Mid-Cayman Rise. *Geochem. Geophys. Geosyst.* **14**, 317–327 (2013).
5. L. A. Levin *et al.*, Hydrothermal vents and methane seeps: Rethinking the sphere of influence. *Front. Mar. Sci.* **3**, 72 (2016).
6. E. B. Sherr, B. F. Sherr, Bacterivory and herbivory: Key roles of phagotrophic protists in pelagic food webs. *Microb. Ecol.* **28**, 223–235 (1994).
7. B. Cho, S. Na, D. Choi, Active ingestion of fluorescently labeled bacteria by mesopelagic heterotrophic nanoflagellates in the East Sea, Korea. *Mar. Ecol. Prog. Ser.* **206**, 23–32 (2000).
8. E. Rocke, M. G. Pachiadaki, A. Cobban, E. B. Kujawinski, V. P. Edgcomb, Protist community grazing on prokaryotic prey in deep ocean water masses. *PLoS One* **10**, e0124505 (2015).
9. M. G. Pachiadaki *et al.*, In situ grazing experiments apply new technology to gain insights into deep-sea microbial food webs. *Deep Sea Res. Part 2 Top. Stud. Oceanogr.* **129**, 223–231 (2016).
10. L. E. Medina *et al.*, A review of protist grazing below the photic zone emphasizing studies of oxygen-depleted water columns and recent applications of in situ approaches. *Front. Mar. Sci.* **4**, 105 (2017).
11. C. L. Van Dover, B. Fry, Microorganisms as food resources at deep-sea hydrothermal vents. *Limnol. Oceanogr.* **39**, 51–57 (1994).
12. M. S. Atkins, A. P. Teske, O. R. Anderson, A survey of flagellate diversity at four deep-sea hydrothermal vents in the Eastern Pacific Ocean using structural and molecular approaches. *J. Eukaryot. Microbiol.* **47**, 400–411 (2000).
13. E. B. Small, M. E. Gross, Preliminary observations of protistan organisms, especially ciliates, from the 21 N hydrothermal vent site. *Bull. Biol. Soc. Wash.* **6**, 401–410 (1985).
14. V. P. Edgcomb, D. T. Kysela, A. Teske, A. de Vera Gomez, M. L. Sogin, Benthic eukaryotic diversity in the Guaymas Basin hydrothermal vent environment. *Proc. Natl. Acad. Sci. U.S.A.* **99**, 7658–7662 (2002).
15. P. López-García, A. Vereschkaka, D. Moreira, Eukaryotic diversity associated with carbonates and fluid-seawater interface in Lost City hydrothermal field. *Environ. Microbiol.* **9**, 546–554 (2007).
16. P. López-García, H. Philippe, F. Gail, D. Moreira, Autochthonous eukaryotic diversity in hydrothermal sediment and experimental microcolonizers at the Mid-Atlantic Ridge. *Proc. Natl. Acad. Sci. U.S.A.* **100**, 697–702 (2003).
17. S. A. Murdock, S. K. Juniper, Hydrothermal vent protistan distribution along the Mariana arc suggests vent endemics may be rare and novel. *Environ. Microbiol.* **21**, 3796–3815 (2019).
18. A. Pasulka, *et al.*, SSU rRNA gene sequencing survey of benthic microbial eukaryotes from Guaymas Basin hydrothermal vent. *J. Eukaryot. Microbiol.* **66**, 637–653 (2019).
19. K. L. Von Damm *et al.*, Chemistry of vent fluids and its implications for subsurface conditions at Sea Cliff hydrothermal field, Gorda Ridge. *Geochem. Geophys. Geosyst.* **7**, Q05005 (2006).
20. D. S. S. Lim *et al.*, SUBSEA 2019 expedition to the Gorda Ridge. *Oceanography* **33**, 36 (2020).
21. D. A. Clague, J. B. Paduan, D. W. Caress, J. McClain, R. A. Zierenberg, Lava flows erupted in 1996 on North Gorda Ridge segment and the geology of the nearby Sea Cliff hydrothermal vent field from 1-M resolution AUV mapping. *Front. Mar. Sci.* **7**, 27 (2020).
22. V. Milesi *et al.*, Forward geochemical modeling as a guiding tool during exploration of Sea Cliff hydrothermal field, Gorda Ridge. *Planet. Space Sci.* **197**, 105151 (2021).
23. T. Fenchel, *Ecology of Protozoa: The Biology of Free-Living Phagotrophic Protists* (Springer-Verlag, 2013).
24. V. P. Edgcomb, M. Pachiadaki, Ciliates along oxyclines of permanently stratified marine water columns. *J. Eukaryot. Microbiol.* **61**, 434–445 (2014).
25. C. Lawerence, S. Menden-Deuer, Drivers of protistan grazing pressure: Seasonal signals of plankton community composition and environmental conditions. *Mar. Ecol. Prog. Ser.* **459**, 39–52 (2012).
26. C. Marrasé, E. Lim, D. Caron, Seasonal and daily changes in bacterivory in a coastal plankton community. *Mar. Ecol. Prog. Ser.* **82**, 281–289 (1992).
27. Y. Morono *et al.*, Carbon and nitrogen assimilation in deep subseafloor microbial cells. *Proc. Natl. Acad. Sci. U.S.A.* **108**, 18295–18300 (2011).
28. M. Mars Brisbin, A. E. Conover, S. Mitarai, Influence of regional oceanography and hydrothermal activity on protist diversity and community structure in the Okinawa Trough. *Microb. Ecol.* **80**, 746–761 (2020).
29. J. A. Huber *et al.*, Isolated communities of *Epsilonproteobacteria* in hydrothermal vent fluids of the Mariana Arc seamounts. *FEMS Microbiol. Ecol.* **73**, 538–549 (2010).
30. V. P. Edgcomb *et al.*, Comparison of Niskin vs. *in situ* approaches for analysis of gene expression in deep Mediterranean Sea water samples. *Deep Sea Res. Part 2 Top. Stud. Oceanogr.* **129**, 213–222 (2016).
31. D. Lynn, *The Ciliated Protozoa: Characterization, Classification, and Guide to the Literature* (Springer Science & Business Media, 2008).

32. F. Zhao, K. Xu, Molecular diversity and distribution pattern of ciliates in sediments from deep-sea hydrothermal vents in the Okinawa Trough and adjacent sea areas. *Deep Sea Res. Part I Oceanogr. Res. Pap.* **116**, 22–32 (2016).

33. R. A. Beinart, D. J. Beaudoin, J. M. Bernhard, V. P. Edgcomb, Insights into the metabolic functioning of a multipartner ciliate symbiosis from oxygen-depleted sediments. *Mol. Ecol.* **27**, 1794–1807 (2018).

34. T. Fenchel, T. Perry, A. Thane, Anaerobiosis and symbiosis with bacteria in free-living ciliates. *J. Protozool.* **24**, 154–163 (1977).

35. C. R. Giner *et al.*, Marked changes in diversity and relative activity of picoeukaryotes with depth in the world ocean. *ISME J.* **14**, 437–449, 10.1038/s41396-019-0506-9 (2019).

36. R. Massana, R. Terrado, I. Forn, C. Lovejoy, C. Pedrós-Alió, Distribution and abundance of uncultured heterotrophic flagellates in the world oceans. *Environ. Microbiol.* **8**, 1515–1522 (2006).

37. A. Schoenle *et al.*, Global comparison of bicosoecid *Cafeteria*-like flagellates from the deep ocean and surface waters, with reorganization of the family *Cafeteriaeae*. *Eur. J. Protistol.* **73**, 125665 (2020).

38. C. de Vargas *et al.*, Ocean plankton. Eukaryotic plankton diversity in the sunlit ocean. *Science* **348**, 1261605–1261605 (2015).

39. L. Guillou *et al.*, Widespread occurrence and genetic diversity of marine parasitoids belonging to *Syndiniales* (Alveolata). *Environ. Microbiol.* **10**, 3349–3365 (2008).

40. D. Moreira, P. López-García, Are hydrothermal vents oases for parasitic protists? *Trends Parasitol.* **19**, 556–558 (2003).

41. Z. D. Kurtz *et al.*, Sparse and compositionally robust inference of microbial ecological networks. *PLoS Comput. Biol.* **11**, e1004226 (2015).

42. J. Pernthaler, Predation on prokaryotes in the water column and its ecological implications. *Nat. Rev. Microbiol.* **3**, 537–546 (2005).

43. K. Simek *et al.*, Morphological and compositional shifts in an experimental bacterial community influenced by protists with contrasting feeding modes. *Appl. Environ. Microbiol.* **63**, 587–595 (1997).

44. M. W. Hahn, M. G. Höfle, Flagellate predation on a bacterial model community: Interplay of size-selective grazing, specific bacterial cell size, and bacterial community composition. *Appl. Environ. Microbiol.* **65**, 4863–4872 (1999).

45. M. W. Hahn, E. R. Moore, M. G. Höfle, Bacterial filament formation, a defense mechanism against flagellate grazing, is growth rate controlled in bacteria of different phyla. *Appl. Environ. Microbiol.* **65**, 25–35 (1999).

46. J. A. Breier *et al.*, A large volume particulate and water multi-sampler with *in situ* preservation for microbial and biogeochemical studies. *Deep Sea Res. Part I Oceanogr. Res. Pap.* **94**, 195–206 (2014).

47. J. S. Seewald, K. W. Doherty, T. R. Hammar, S. P. Liberatore, A new gas-tight isobaric sampler for hydrothermal fluids. *Deep Sea Res. Part I Oceanogr. Res. Pap.* **49**, 189–196 (2002).

48. B. F. Sherr, E. B. Sherr, R. D. Fallon, Use of monodispersed, fluorescently labeled bacteria to estimate *in situ* protozoan bacterivory. *Appl. Environ. Microbiol.* **53**, 958–965 (1987).

49. E. Trembath-Reichert, D. A. Butterfield, J. A. Huber, Active subseafloor microbial communities from Mariana back-arc venting fluids share metabolic strategies across different thermal niches and taxa. *ISME J.* **13**, 2264–2279 (2019).

50. D. A. Caron, Protistan herbivory and bacterivory. *Methods Microbiol.* **30**, 289–315 (2001).

51. J. Salat, C. Marrasé, Exponential and linear estimations of grazing on bacteria: Effects of changes in the proportion of marked cells. *Mar. Ecol. Prog. Ser.* **104**, 205–209 (1994).

52. T. Stoeck *et al.*, Multiple marker parallel tag environmental DNA sequencing reveals a highly complex eukaryotic community in marine anoxic water. *Mol. Ecol.* **19** (suppl. 1), 21–31 (2010).

53. S. K. Hu, P. E. Connell, L. Y. Mesrop, D. A. Caron, A hard day's night: Diel shifts in microbial eukaryotic activity in the north pacific subtropical gyre. *Front. Mar. Sci.* **5**, 351 (2018).

54. C. S. Fortunato, B. Larson, D. A. Butterfield, J. A. Huber, Spatially distinct, temporally stable microbial populations mediate biogeochemical cycling at and below the seafloor in hydrothermal vent fluids. *Environ. Microbiol.* **20**, 769–784 (2018).

55. J. G. Caporaso *et al.*, Ultra-high-throughput microbial community analysis on the Illumina HiSeq and MiSeq platforms. *ISME J.* **6**, 1621–1624 (2012).

56. A. Apprill, S. McNally, R. Parsons, L. Weber, Minor revision to V4 region SSU rRNA 806R gene primer greatly increases detection of SAR11 bacterioplankton. *Aquat. Microb. Ecol.* **75**, 129–137 (2015).

57. A. E. Parada, D. M. Needham, J. A. Fuhrman, Every base matters: Assessing small subunit rRNA primers for marine microbiomes with mock communities, time series and global field samples. *Environ. Microbiol.* **18**, 1403–1414 (2016).

58. J. G. Caporaso *et al.*, Global patterns of 16S rRNA diversity at a depth of millions of sequences per sample. *Proc. Natl. Acad. Sci. U.S.A.* **108** (suppl. 1), 4516–4522 (2011).

59. E. Bolyen *et al.*, Author correction: Reproducible, interactive, scalable and extensible microbiome data science using QIIME 2. *Nat. Biotechnol.* **37**, 1091 (2019).

60. B. J. Callahan *et al.*, DADA2: High-resolution sample inference from Illumina amplicon data. *Nat. Methods* **13**, 581–583 (2016).

61. L. Guillou *et al.*, The Protist Ribosomal Reference database (PR2): A catalog of unicellular eukaryote small sub-unit rRNA sequences with curated taxonomy. *Nucleic Acids Res.* **41**, D597–D604 (2013).

62. Q. Wang, G. M. Garrity, J. M. Tiedje, J. R. Cole, Naive Bayesian classifier for rapid assignment of rRNA sequences into the new bacterial taxonomy. *Appl. Environ. Microbiol.* **73**, 5261–5267 (2007).

63. C. Quast *et al.*, The SILVA ribosomal RNA gene database project: Improved data processing and web-based tools. *Nucleic Acids Res.* **41**, D590–D596 (2013).

64. A. R. Coenen, S. K. Hu, E. Luo, D. Muratore, J. S. Weitz, A primer for microbiome time-series analysis. *Front. Genet.* **11**, 310 (2020).

65. G. B. Gloor, J. M. Macklaim, V. Pawlowsky-Glahn, J. J. Egoscue, Microbiome datasets are compositional: And this is not optional. *Front. Microbiol.* **8**, 2224 (2017).

66. L. Tipton *et al.*, Fungi stabilize connectivity in the lung and skin microbial ecosystems. *Microbiome* **6**, 12 (2018).

67. S. K. Hu, Gorda Ridge data analysis. GitHub. <https://shu251.github.io/protist-gordaridge-2021>. Deposited 2 January 2021.

68. S. K. Hu, Ridge data analysis. GitHub. <https://github.com/shu251/protist-gordaridge-2021>. Deposited 28 June 2021.